

## **Roughness, Hardness and Giant Magneto Resistance of Cu/Co Multilayers Prepared by Jet electrochemical deposition**

Wei Jiang<sup>1</sup>, Lida Shen<sup>1</sup>, Mingyang Xu, Jun Zhu, Zongjun Tian\*

College of Mechanical and Electrical Engineering, Nanjing University of Aeronautics and Astronautics, Yu Dao Street, 210016 Nanjing, China

<sup>1</sup>These authors contributed equally to this work.

\*E-mail: [tianzj@nuaa.edu.cn](mailto:tianzj@nuaa.edu.cn)

*Received:* 21 May 2018 / *Accepted:* 18 July 2018 / *Published:* 1 September 2018

---

Cu/Co multilayer film was prepared on a Si substrate using a translational jet electrochemical deposition system. A scanning electron microscope, X-ray diffractometer, a 3D surface profilometer, a digital microhardness tester, and a physical property measurement system were used to characterize the surface topography, microtexture, roughness, microhardness, and giant magnetoresistance respectively. It was found that the surface morphology of the multilayer improved and the interface between the Cu and Co layers was well-defined. The roughness and hardness of the multilayer are superior to those of single metal film. The Cu/Co multilayer exhibited an excellent giant magnetoresistive ratio of 50.38%. The giant magnetoresistance increased with the increase in the multilayer cycle number and decreased when the cycle number exceeded 120. The multilayer prepared by this method has high sensitivity to magnetoresistive change and it is easy to control the multilayer's resistance.

---

**Keywords:** jet electrochemical deposition; Cu/Co multilayer; Giant Magnetoresistance

### **1. INTRODUCTION**

Multilayers are developed using individual single-layer films. A multilayer structure is obtained by alternately depositing the films in the direction of growth [1-6]. Yao prepared Cu/Ni multilayers using a single-groove method and double-groove method and compared the performances of the multilayers [7]. It was demonstrated that both methods have advantages and disadvantages and are complementary. Peter used a computer-controlled galvanostatic/potentiostatic (G/P) method to create Co-Ni-Cu/Cu multilayers [8]. Dulal used a flow tank (the plating liquid flowed into the tank), constant voltage, and a double pulse power supply to create Co-Ni-Cu/Cu multilayers [9]. Dhirendra investigated the composition modulation in Cu/Co multilayers grown by a pulse train-based deposition technique [10]. Highly uniform Co/Cu multilayer nano-wire arrays were electrodeposited into nano-

channels of porous anodic aluminum oxide template [11]. Liu investigated the structure and magnetic properties of multilayers on different substrates using a radio frequency (RF) magnetron sputtering technique [12].

To date, many researchers have used magnetron sputtering or slot-plating methods to prepare multilayers. However, magnetron sputtering is expensive and the requirements are complex. Slot plating suffers from cross-contamination and has low processing efficiency. Our team has studied jet electrochemical deposition for 10 years [13-19]. Unlike slot plating, jet electrochemical deposition improves the current density and efficiency. Therefore, a translational jet electrochemical deposition system is developed to prepare Cu/Co/Cu multilayers. The system has the advantages of stability, reliability, use of simple equipment, no cross-contamination, and high efficiency. It has been found that this system produces multilayers with high giant magnetoresistance (GMR) and high sensitivity. In addition, the modulation wavelength of the multilayer film can be controlled by alternating the reciprocal deposition.

## 2. EXPERIMENTAL PROCEDURE

### 2.1 Experimental device

Figure 1 shows the translational jet electrochemical deposition system. The system consists of a machine body, translation array injection unit, power supply control system, electrolyte circulation temperature control system, and stepper motor control system. The electrodeposition unit includes a Cu anode with a wash nozzle and a Co anode with a wash nozzle. They are used for depositing the Cu/Co and washing. The workpiece is reciprocally scanned and connected to the cathode. Cu/Co are alternately deposited to form a multilayer film, which must be washed to eliminate pollution during the alternating deposition.

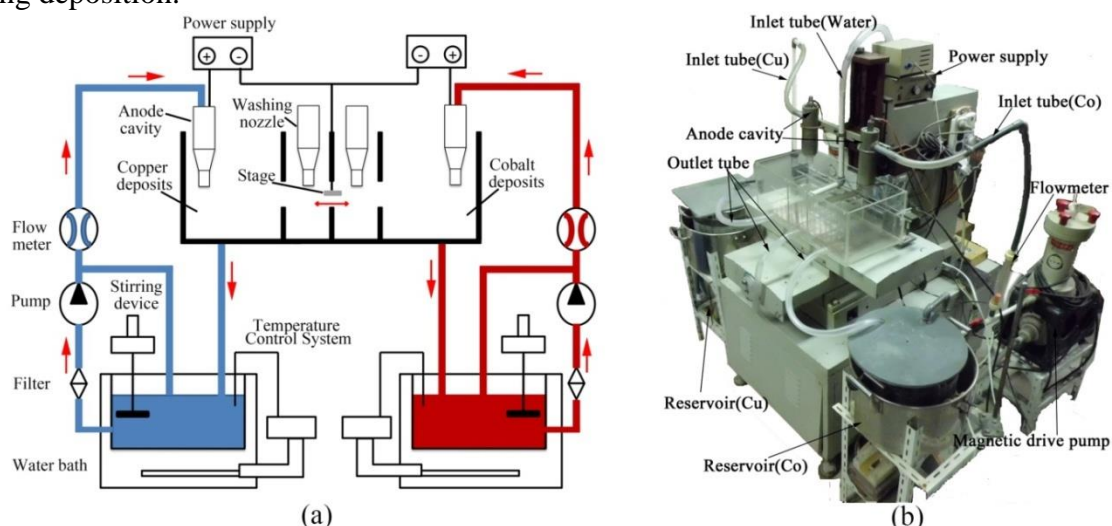


**Figure 1.** Multiplexed translational jet electrochemical deposition system

A schematic diagram of the Cu/Co multilayer deposition is shown in Figure 2. In this experiment, the Cu/Co multilayers were prepared using the translational jet electrochemical deposition

system. For the copper deposition, the flowing electrolyte continuously transports  $\text{Cu}^{2+}$  to the substrate's surface. Under the action of an external electric field, the electrons of  $\text{Cu}^{2+}$  are adsorbed onto the surface to form Cu. The copper was deposited first followed by the cobalt. During this process, the multilayer film grows steadily.

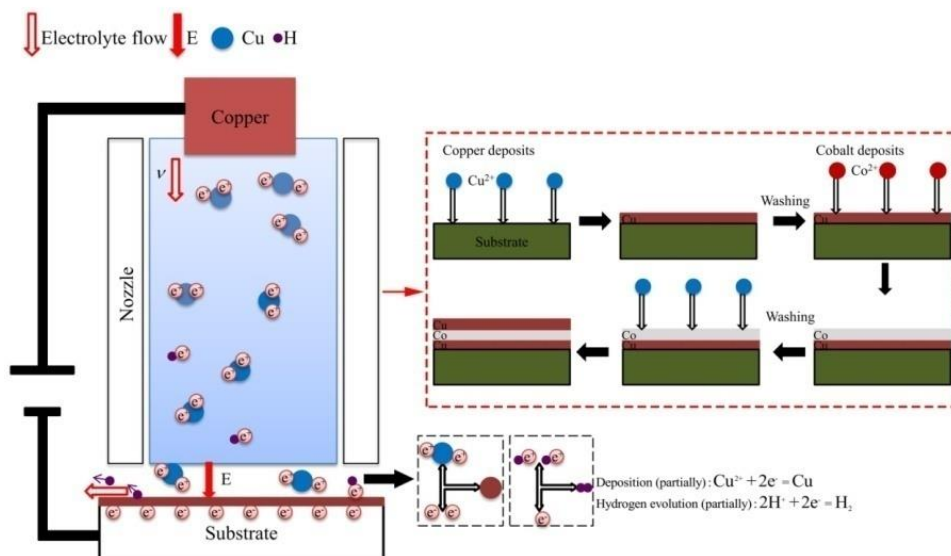


**Figure 2.** Schematic of the preparation of the Cu/Co multilayers by jet electrochemical deposition

### 2.2 Experimental parameters

The reagents were analytically pure. The Cu solution consists of  $\text{CuSO}_4 \cdot 5\text{H}_2\text{O}$  (250g/L) and  $\text{H}_2\text{SO}_4$  (50g/L) and the solution temperature is 30 °C. The Co solution consists of  $\text{CoSO}_4 \cdot 6\text{H}_2\text{O}$  (280g/L),  $\text{CoCl}_2 \cdot 6\text{H}_2\text{O}$  (38g/L), and  $\text{H}_3\text{BO}_3$  (40g/L) and the solution temperature is 50 °C. The substrate material is monocrystalline silicon ( $25 \times 25 \times 4$  mm). The surface of the substrate requires polishing, degreasing, pickling-activation, and other pretreatments. The experimental parameters are shown in Table 1.

**Table 1.** Experimental parameters

Project	Parameters
Scan times	100
Translational velocity	10mm/s
Electrolyte flow rate	250L/h
Machining gap	2mm
Current density (Cu/Co)	80A/dm <sup>2</sup>

### 2.3 Characterization of the multilayer film

The instruments and parameters for the characterization of the multilayer film are shown in Table 2.

**Table 2.** Instruments and parameters

Characterization	Instruments(Type)
Microscopic morphology	SEM(S-3400)
Structure analysis	XRD (D/max 2500VL/PC)
Roughness	3D Surface Profilometer(MicroXAM-100)
Microhardness	Digital microhardness tester(HVS-1000A)
Giant Magneto Resistance	Physical Property Measurement System(KT-20)

### 3. RESULTS AND DISCUSSION

#### 3.1 Surface morphology and microtexture

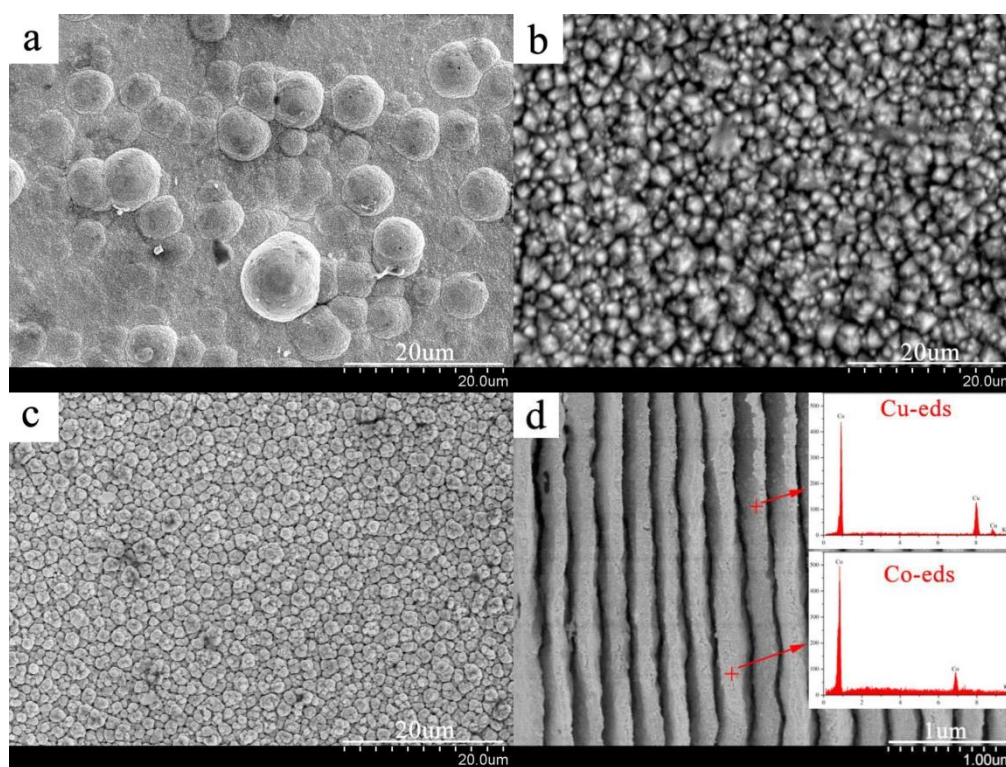


**Figure 3.** Surface and cross-section morphology of the film

Figure 3 shows the surface and cross-section morphology of the film obtained by jet electrochemical deposition. Figure 3a shows the Cu film with many cellular protuberances on the surface. Figure 3b shows the Co film, which exhibits a sharp tetrahedral corner protuberance; the Co film is denser than the Cu film. Figure 3c shows the Cu/Co multilayer with a uniform cell and without cellular protuberances distribution on the surface. It is observed that the surface morphology of the Cu/Co multilayer is better than that of the single layers and this is related to the alternate deposition of the copper and cobalt. The monolayer thickness is at the nanoscale during the alternate deposition and if the grains do not grow and aggregate, the next deposition period begins, this increases the discharge

activation point. It is preferred to obtain films with small grains, dense texture, and good surface quality.

In order to observe the Cu/Co multilayer structure and considering the resolution of the scanning electron microscope (SEM-S3400), the magnification was set to 10X (the theoretical thickness is increased about 10 times). Figure 3d shows the cross-section morphology of the Cu/Co multilayers and the energy dispersive spectroscopy (EDS) results. The multilayer exhibits a good periodic structure and the interface between the copper film and the cobalt film is distinct and straight. This is due to the alternate deposition of the copper and cobalt coatings that affects the changes in the crystal structure and the surface quality of the multilayer film.

The X-ray diffraction (XRD) patterns of the Cu/Co multilayer is shown in Figure 4. The Cu and Co peaks are located close to each other. The preferred orientations of multilayer films are (111) and (220). The multilayer film grows in two directions. By reducing the differences in the growth at different points, the crystals of the film are even, thereby improving the film density. In addition, the Cu and Co peaks are fused to each other and form a satellite peak, which further demonstrates that the multilayer prepared by this method is structurally complete and has a good periodic structure [25].

In general, the film prepared by jet electrodeposition is island grown and the surface of the film shows different degrees of cellular protuberances [18, 19]. In this study, the selective scanning motion of the nozzle is perpendicular to the silicon substrate. The migrating ions are concentrated in the discharge deposition under the nozzle, which creates the conditions for the stratified growth at the beginning of the jet electrodeposition. As shown in Figure 4, the Cu-Co multilayer prepared on the silicon substrate has two preferred orientations, which illustrates the characteristics of the layered growth and reduces the difference in the crystal growth rate at different locations [26]. Therefore, it can be concluded that the multilayer film deposited by jet electrodeposition on silicon substrate are mainly layered.

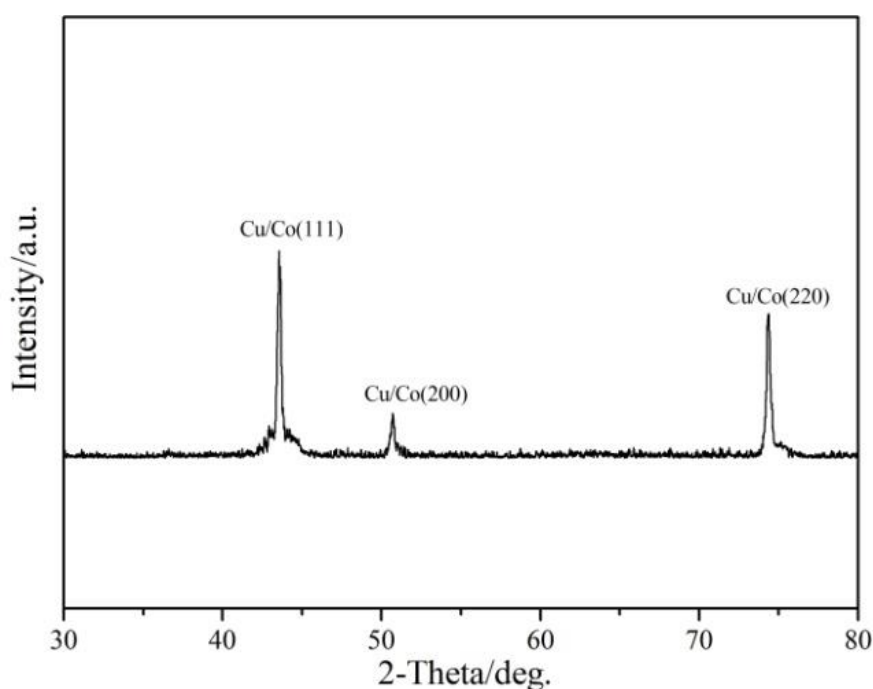


**Figure 4.** The XRD pattern of the Cu/Co multilayer

### 3.2 Roughness and microhardness

Figure 5 shows the surface roughness and microhardness of the pure Cu, pure Co, and the Cu/Co multilayer. The multilayer surface roughness is low at 0.167  $\mu\text{m}$ . The jet electrochemical deposition involves partial scanning. Therefore, each deposition represents a new discharge activation process and this approach is conducive to the formation of a fine-grained, dense microstructure. At the same time, the high velocity of the jet electrochemical deposition reduces the thickness of the diffusion layer and ensures the transport of solutes, which reduces the concentration polarization and results in a high-quality film. In addition, due to the alternate deposition of the different elements, there is an interface effect and the crystal structure changes such as doping and infiltration are conducive to the reduction in the surface roughness.

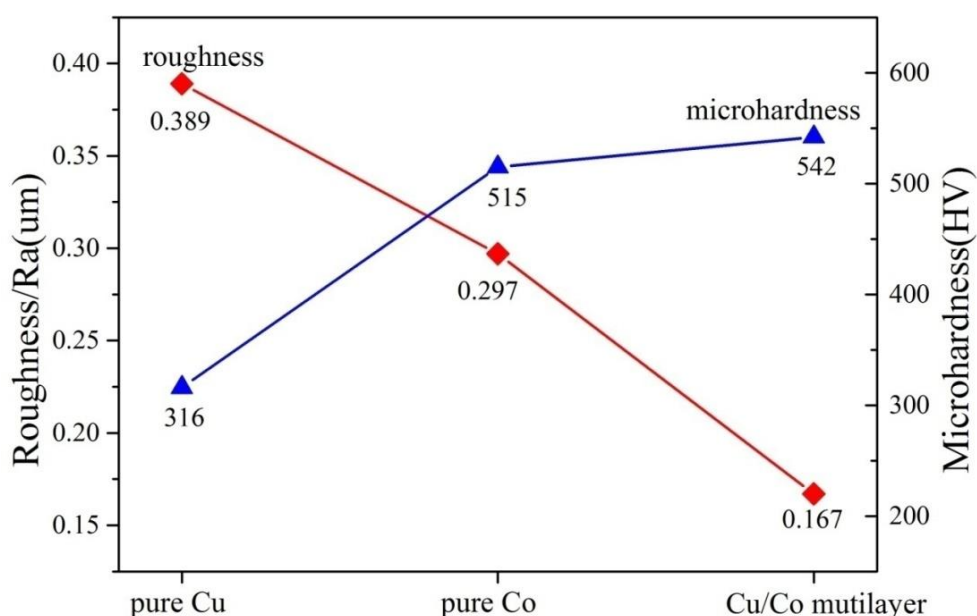


**Figure 5.** Roughness and microhardness of the film

The microhardness of the Cu/Co multilayer is 542 HV and the reason for the high hardness is the alternate deposition of the Cu and Co layers [20, 21]. At the interface of the Cu and Co layers, misfit dislocations are generated due to the different lattice constants and atomic sizes of the Cu and Co, this causes stress between the film layers. This stress improves the hardness and improves the strength of the multilayer film. [22, 23]. In addition, the multilayer’s microstructure and properties, such as grain morphology, crystal structure, grain size, and orientation also have important influences on the roughness and microhardness [24].

### 3.3 GMR

The reluctance change rate  $\Delta R/R$  is defined as  $\Delta R/R = (R_{\text{max}} - R_{\text{min}}) \times 100\%/R_{\text{min}}$  where  $R_{\text{max}}$  is the resistance when there is no magnetic field and  $R_{\text{min}}$  is the resistance under the applied field [27, 33].

Figure 6 shows the exchange coupling of the magnetization direction and the magnetoresistance curve of the Cu/Co multilayer [28, 29]. The electrodeposition of the Cu/Co scans per unit period is equal, 120 times in total. The Cu/Co multilayer exhibits the largest resistance without a magnetic field, whereas the resistance decreases rapidly under a magnetic field. The multilayer's resistance reaches a minimum value when the magnetic field strength is 600 Oe and the curve tends to stabilize when the magnetic field of the multilayer is in the same direction as the applied electric field [34-37]. Figure 6 shows that  $R_{\max}$  is 0.594  $\Omega$ ,  $R_{\min}$  is 0.395  $\Omega$ , and the GMR ratio of the Cu/Co multilayer is 50.38%, indicating that the use of this method results in a GMR effect in the multilayer. In addition, we also find that the Cu/Co multilayer is saturated at a magnetic field strength of 1000 Oe, its resistance is reduced, and the magnetoresistive variation with high sensitivity can be controlled easily.

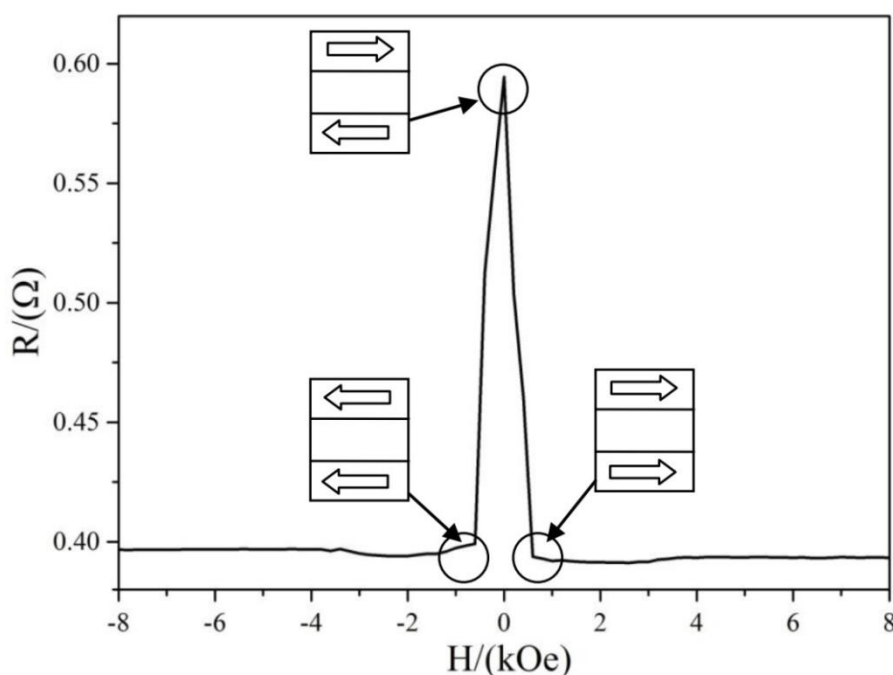


**Figure 6.** Exchange coupling of the magnetization direction and magnetoresistance curve of the Cu/Co multilayer

### 3.3.1 Effect of multilayer cycle number on GMR

Figure 7 shows that the GMR of the Cu/Co multilayer increase and then decreases as the cycle number increases. The GMR reaches the maximum of 50.38% when the cycle number is 120. According to the principle of GMR, an increase in the cycle number increases the resistance in an anti-parallel magnetization state but has little effect on the resistance in a parallel magnetization state [38]. When the cycle number exceeds 120, the GMR decreases as the number of cycles increases. In this study, the increase in the number of cycles means that the thickness of the coating increases, that is, the GMR is indirectly related to the thickness of the coating. Jet electrodeposition studies have shown that crystal defects increase with the thickening of the coating [16, 17]. In addition, the high current density of jet electrochemical deposition amplifies the defects, which has a large influence on the multilayer

structure with a single layer thickness of only a few nanometers, this may cause a magnetic short circuit, resulting in a decrease in the GMR [39].

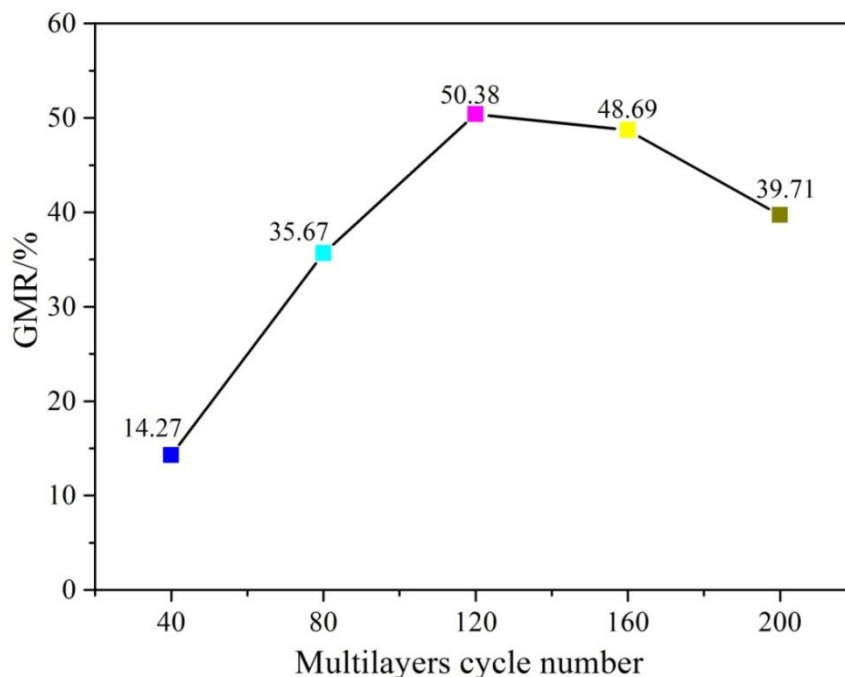


**Figure 7.** GMR of the Cu/Co multilayer for different cycle numbers

### 3.3.2 Effect of the number of Co scans per period on the GMR

In order to determine the effect of the thickness of the Co layer on the multilayer GMR during the modulation period of the multilayer film, the following experiment was performed. Assuming that the Cu layer thickness is approximately equal to the thickness of the Co layer for the same number of scans and the number of cycles is set to 200, the number of Co scans was gradually increased to prepare Cu:Co multilayers at different ratios (1:1, 1:2, 1:3, 1:4, and 1:5).

Figure 8 shows the changes in the multilayer's GMR for the different Cu-Co scan ratios; the results indicate that the GMR decreases with the increase in the number of Co scans. The generation of the GMR is directly related to the scattering of the conductive electrons by the Co layer. However, the GMR is reduced as the cobalt layer is thickened. Based on the microstructure analysis of the multilayer, the interface of the Cu/Co multilayer has a specific form and the inverse relationship between the GMR and the Co thickness demonstrates the scattering of the electrons during antiparallel magnetization. The dominant influencing factor is the interface layer that contains copper and cobalt rather than the Co layer. The proportion of the interface layer decreases as the thickness of the Co layer increases, and the GMR decreases. In addition, the decrease in the coating quality as the plating thickness increases also has a certain influence on the GMR [40-41].

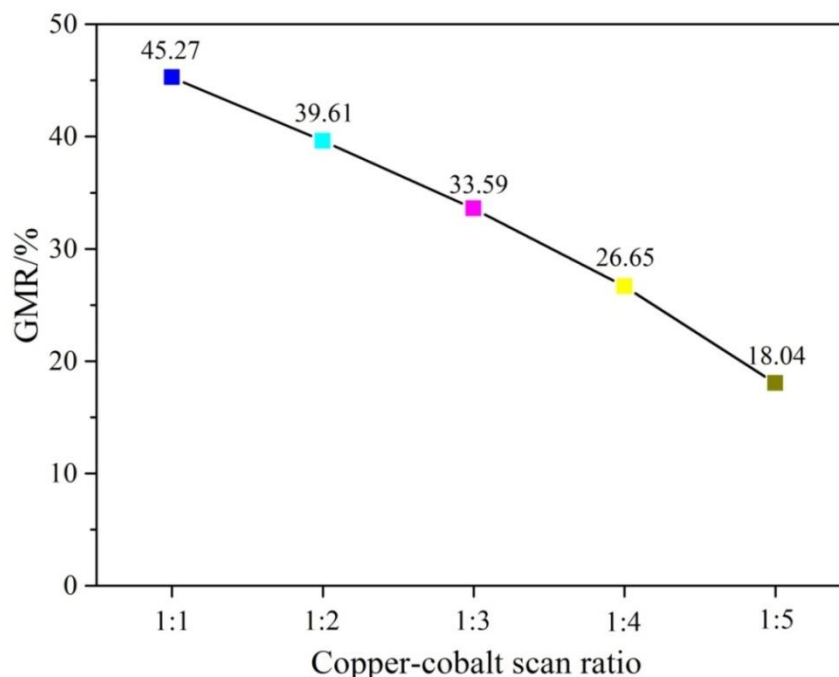


**Figure 8.** Changes in the multilayer's GMR for different Cu-Co scan ratios

### 3.3.3 Effect of current density on the GMR of the Copper-Cobalt Multilayer

In order to investigate the effect of different electrodeposition parameters on the GMR of the multilayer [42], the thickness ratio of the copper and cobalt is set to 1: 1, the scanning speed is 10 mm/s, and the current density is changed to regulate the growth of the multilayer. Figure 9 shows the changes in the GMR of the Cu-Co multilayer at different current densities. It is observed that the maximum GMR of the multilayer film is 50.38% at a current density of 80 A/dm<sup>2</sup> and the current density shows a decreasing trend with increasing amplitude. However, the GMR tends to decrease when the current density increases. The reason is that the current density is the key factor determining (Discharge growth) of the jet electrodeposition. Because of its specific fluid flow characteristics and strong mass transfer, the current density on the cathode surface directly affects the film's surface quality. In jet electrodeposition, when the electrolyte flow rate is constant and the current density is low, the ions involved in the reaction on the cathode surface in the electrolyte can be replenished in time and the ion reaction concentration is stable; therefore, the coating surface is flat. However, when the current density is high, the edge discharge effect of the jet electrodeposition is aggravated, resulting in a lower surface smoothness of the coating [30-31]. Therefore, by selecting the appropriate current density, a dense coating, fine grain, and improved performance are achieved. In order to minimize the increase in the edge discharge, pulse electrodeposition [30], friction composite electrodeposition [15,32], and rotating interleaving electrodeposition [31] can be used to improve the quality and performance of the coating.

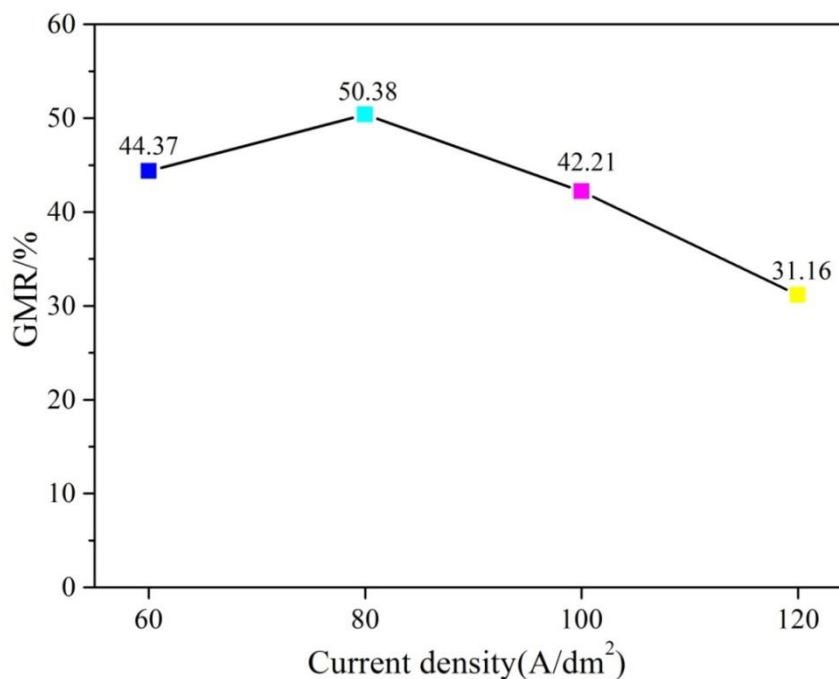


**Figure 9.** Effect of the current density of jet electrodeposition on GMR

#### 4. CONCLUSIONS

(1) The Cu/Co multilayer created by multivariate translational jet electrochemical deposition has good surface morphology, the growth interface is clear, and the two orientation surfaces are (111) and (220).

(2) The alternating deposition of copper and cobalt causes a redistribution of the discharge on the cathode surface, which is conducive to a fine-grained texture, dense coating, and the improvement of the surface roughness and hardness.

(3) The increase in the cycle number results in an increase in the resistance in an anti-parallel magnetization state. The Cu/Co multilayer exhibits an excellent giant magnetoresistive ratio of 50.38%.

(4) The GMR of the Cu/Co multilayer decreases with the increase in the number of Co scans. As the Co layer thickness increases, the proportion of the interfacial layer decreases and the GMR decreases in inverse proportion. In an anti-parallel magnetization state, the Cu/Co interfacial layer plays a dominant role in electron scattering.

#### ACKNOWLEDGEMENTS

The authors greatly acknowledge financial support from National Natural Science Foundation of China (Grant No. 51475235, No. 51105204 and No. U1537105). We also extend our sincere thanks to all who contributed in the preparation of these instructions.

#### References

1. F. Xu, Y.N. Lv, Y. Xie and F.Y. Liu, *Corros. Sci. Prot. Technol.*, 20 (2008) 32.

2. J.Y. Fei and G.D. Wilcox, *Surf. Coat. Technol.*, 200 (2006) 3533.
3. J. Tan, H.J. Y and W.C. Guo, *Mater. Rev.*, 19 (2005) 191.
4. F. Gui and S.W. Yao, *Electroplat. Pollut. Control.*, 20 (2000) 3.
5. Y.X Yan, J.X Zhang, Y.Y. Fan and J.H. Zhang, *Electroplat. Pollut. Control.*, 5 (2008) 1.
6. Q.A. Huang, Y.P. Wang, K. Zhang, Y.M. Zhang, Y.Y. Chen and J.X. Yu, *Electroplat. Finishing.*, 17 (1998) 48.
7. S.W. Yao, F. Gui, W.G. Zhang, Z.Y. Feng and S.P. Dou, *J. Tianjin. Univ.*, 34 (2001) 261.
8. L. Peter, G.L. Katona, Z. Berenyi, K. Vad, G.A. Langer, E. Toth-Kadar, J. Padar, L. Pogany and I. Bakonyi, *Electrochim. Acta.*, 53 (2007) 837.
9. S.M.S.I. Dulal and E.A. Charles, *J. Alloy. Compd.*, 455 (2008) 274.
10. D. Gupta, A.C. Nayak, M. Sharma, R.R. Singh, S.K. Kulkarni and R.K. Pandey, *Thin. Solid. Films.*, 513 (2006) 187.
11. Z.X Song, Y.J. Xie, S.W Yao, H.Z. Wang, W.G. Zhang and Z.Y. Tang, *Mater. Lett.*, 65 (2011) 1562.
12. H.L. Liu, W.J. Li, J.H. Yang, M. Gao, X.Y. Liu and M.B. Wei, *J. Mater. Sci-Mater. El.*, 3 (2017) 2949.
13. J. Zhu, Z.J. Tian, Z.D. Liu, L.D. Shen and Y.H. Huang, *J. South. China. Univ. Techno.*, 39 (2011) 92.
14. L.D. Shen, Y.H. Wang, W. Jiang, X. Liu, C. Wang and Z.J. Tian, *Corros. Eng. Sci. Techn.*, 52 (2017) 311.
15. X. Liu, L.D. Shen, M.B. Qiu, Z.J. Tian, Y.H. Wang and K.L. Zhao, *Surf. Coat. Tech.*, 305 (2016) 231.
16. G.F. Wang, L.D. Shen and Y.H. Huang, *Int. J. Electrochem. Sc.*, 7 (2012) 10818.
17. Y.H. Wang, L.D. Shen, M.B. Qiu, Z.J. Tian, X. Liu and W. Zhuo, *J. Electrochem. Soc.*, 163 (2016) 579.
18. W. Zhuo, L.D. Shen, M.B. Qiu, Z.J. Tian and W. Jiang, *Surf. Coat. Tech.*, 333 (2017) 87.
19. C. Wang, L.D. Shen, M.B. Qiu, Z.J. Tian and W. Jiang, *J. Alloy. Compd.*, 727 (2017) 269.
20. A. Misra, J.P. Hirth and R.G. Hoagland, *Acta. Materialia.*, 53 (2005) 4817.
21. J. Wang and A. Misra, *Curr. Opin. Solid. ST. M.*, 15 (2011) 20.
22. D. Cheng, Z.J. Yan and L. Yan, *Acta. Metall. Sin.*, 42 (2006) 118.
23. Y. Liu, D. Bufford, H. Wang, C. Sun and X. Zhang, *Acta. Materialia.*, 59 (2011) 1924.
24. X.X. Wei, C. Song, K.W. Geng, F. Zeng, B. He and F. Pan, *J. Phys-Condens. Mat.*, 18 (2006) 7471.
25. K. Neurohr, L. Peter, L. Pogany, D. Rafaja, A. Csik, K. Vad, G. Molnar and I. Bakonyi, *J. Electrochem. Soc.*, 163 (2015) 485.
26. B.G. Toth, L. Peter, J. Degi, A. Revesz, D. Oszetzky, G. Molnár and I. Bakonyi, *Electrochim. Acta.*, 91 (2013) 122.
27. A. Cziraki, L. Peter, B. Arnold, J. Thomas, H.D. Bauer, K. Wetzig and I. Bakonyi, *Thin. Solid. Films.*, 424 (2015) 229.
28. J. Mino, V. Zhukova, J.J.D. Val, M. Ipatov, A. Martinez-Amesti, R. Varga, and A. Zhukov, *J. Electron. Mater.*, 45 (2016) 2401.
29. B.G. Toth, L. Peter and I. Bakonyi, *J. Electrochem. Soc.*, 158 (2011) 671.
30. K. Zhao, L. Shen, M. Qiu, Z. Tian and W. Jiang, *Int. J. Electrochem. Sc.*, 12 (2017) 8578.
31. L. Shen, C. Wang, Z. Tian, W. Jiang, W. Zhuo and K. Zhao, *Int. J. Electrochem. Sc.*, 13 (2018) 1831.
32. L. Shen, W. Zhuo, M. Qiu, W. Jiang, K. Zhao and C. Wang, *Mater. Sci. Tech-lond.*, 34 (2017) 419.
33. W.R.A. Meuleman, S. Roy, L. Peter and I. Bakonyi, *J. Electrochem. Soc.*, 151 (2004) 256.
34. S. Kainuma, K. Takayanagi, K. Hisatake and T. Watanabe, *J. Magn. Mater.*, 246 (2002) 207.
35. N. Rajasekaran, J. Mani, B.G. Toth, G. Molnar, S. Mohan, L. Peter and I. Bakonyi, *J. Electrochem. Soc.*, 162 (2015) 204.
36. S.B. Sakrani, Y.B. Wahab and Y.C. Lau, *J. Alloy. Compd.*, 434 (2007) 598.

37. K. Neurohr, L. Peter, L. Pogany, D. Rafaj, A. Csik, K. Vad, G. Molnar, and I. Bakonyi, *J. Electrochem. Soc.*, 162 (2015) 331.
38. S.C. Lima and M.N. Baibich, *J. Appl. Phys.*, 119 (2016) 033902.
39. X.T. Tang, G.C. Wang and M. Shima, *Phys. Rev. B.*, 75 (2007) 134404 .
40. B.G. Toth, L. Peter, L. Pogany, A.Revesz and I. Bakonyi, *J. Electrochem. Soc.*, 161 (2014) 154.
41. N. Rajasekaran, L. Pogany, A. Revesz, B.G. Toth, S. Mohan,b L. Peter and I. Bakonyi, *J. Electrochem. Soc.*, 161 (2014) 339.
42. M. Kuzminski, A. Slawska-Waniewska, H.K. Lachowicz and M. Knobel, *J. Magn. Magn. Mater.*, 205 (1999) 7.

© 2018 The Authors. Published by ESG ([www.electrochemsci.org](http://www.electrochemsci.org)). This article is an open access article distributed under the terms and conditions of the Creative Commons Attribution license (<http://creativecommons.org/licenses/by/4.0/>).